Quantum Phase Transitions in Josephson Junction Arrays [*]

Rosario Fazio[(1)] and Gerd Schön[(2)]

[(1)]*Istituto di Fisica, Università di Catania & INFM, viale A. Doria 6, 95129 Catania - Italy*
[(2)]*Institut für Theoretische Festkörperphysik, Universität Karlsruhe, D 76128 Karlsruhe, Germany*
(October 15, 1997)

Abstract

In this chapter we review the quantum phase transitions and transport properties of low-capacitance Josephson junction arrays. We will present the models and introduce the relevant topological excitations. The phase diagram depends in a very rich way on various control parameters. We will discuss the universality or or absence of universality of the transport properties at the quantum phase transition.

I. INTRODUCTION

Josephson junctions arrays (JJA) are ideal model systems to study a variety of non-conventional phase transitions [1–3]. In the last years, due to the development of the microfabrication techniques, it became possible to fabricate Josephson arrays whose junctions are of submicron size. In these systems the competition of single electron effects [4] with the Josephson effect, leads to a number of quantum phase transitions with a very rich phase diagram. In this chapter we review some theoretical aspects of quantum critical phenomena in these systems. This topic will be also touched in the chapter of J.V. Josè while a review on experiments is given in the chapters of H. van der Zant and P. Delsing.

In JJA it is important to distinguish between local and global superconductivity. When cooling the sample, each island of the array becomes superconducting (develops a nonvanishing gap Δ) at a critical temperature T_c. However, dissipation-less conduction requires phase coherence of the superconducting order parameter $\Delta e^{i\phi_i}$ across the whole system. This can set in at a much lower temperature T_J, which defines the superconducting transition temperature. Alternatively, if the junction are submicron size, the low temperature phase of the array may be insulating even though each island is superconducting [5–7].

The two characteristic energy scales in the system are the Josephson energy E_J which is associated to the tunneling of Cooper pairs between neighboring islands and the charging energy $E_C = e^2/2C$ (where C is the geometrical capacitance of the junction) which is the energy cost to add an extra electron charge to a neutral island. The electrostatic energy inhibits the fluctuations of the charge due to tunneling; equivalently, it enhances the quantum

---

fluctuations of the phases ϕ's of the superconducting order parameters of the islands. If $E_{\mathrm{J}} \gg E_{\mathrm{C}}$ the system turns superconducting at low temperatures since the fluctuations of the ϕ_i's are weak and the system is globally phase coherent. We will refer to the $E_{\mathrm{J}}/E_{\mathrm{C}} \to \infty$ limit as the *classical* case (in the classical limit JJA's are a physical realization of the two dimensional XY-model). In the opposite limit, $E_{\mathrm{J}} \ll E_{\mathrm{C}}$, the array becomes a Mott insulator since the charges Q_i in each islands are localized (Coulomb blockade of Cooper pairs) while strong quantum fluctuations of ϕ_i prevent the system to reach long range phase coherence. At a critical ratio of these coupling energy a superconductor-insulator (SI) transition occurs. It has been observed experimentally by the groups of Delft and Goteborg [5–7].

In the classical limit vortices are the topological excitations which determine the (thermo)dynamic properties of JJA. Deep in the quantum limit ($E_{\mathrm{J}} \ll E_{\mathrm{C}}$) the charges on each island are the relevant degrees of freedom. Vortices and charges play a dual role and many features of JJA can be observed in the two limits if the role of charges and vortices are interchanged [12,13].

Many of the properties discussed here, are also observed in granular superconductors [8] and ultra thin superconducting films [9–11]. In granular systems disorder plays a crucial role, while this is virtually absent in JJAs, or it can be introduced in a controlled way. In ultra-thin films it is believed that pre-formed Cooper pairs exist and that phase fluctuations, which can be controlled by varying the film thickness, drive the system through the SI transition.

It is well established that in classical arrays an applied magnetic field leads to frustration [16], with similar effects predicted for quantum JJAs [14,15]. In a quantum JJA an applied gate voltage relative to the ground plane V_{x} introduces a *charge frustration*. The combination of charge frustration and finite-range Coulomb interaction leads to the appearance of various Mott insulating phases [17]. They are characterized by crystal-like configurations (with a lattice constant which depends on V_{x}) of the charges on the islands. In addition a new phase, characterized by the coexistence of off-diagonal (superconducting) and diagonal (charge-crystalline) long range order, occurs. This phase is known as *supersolid*. The combination of charge *and* magnetic frustration may lead to qualitatively new effects [25]. The most striking prediction is that for certain ratios of the magnetic to charge frustration the JJA is in a Quantum Hall phase [26].

In quantum phase transitions the dynamics and thermodynamics are intimately interconnected. Hence rather peculiar transport properties are expected close to the SI transition. One of the most striking predictions in this respect is that at the transition the conductance is finite and universal [27,28]. Since the original prediction of a metallic behavior at zero temperature for two-dimensional superconductors there has been a substantial interest in the actual value of the universal conductance, and in the possibility of non-universal corrections [29].

This chapter is organized as follows. In the next section the models which are used to study quantum JJA will be introduced. Although different in many details, all those models have similar phase diagrams. In section III some theoretical tools to study the phase diagram are briefly discussed: the mean field approximation, the coarse graining approach to derive a Ginzburg-Landau effective free energy, and the Villain transformation which leads to a description in terms of charges and vortices. These approaches capture most of the essential physics. The subsequent section is devoted to a description of the phase diagram including the case when there is charge and/or magnetic frustration. Since the number of parameters

which can be varied is rather large, the phase diagram is discussed only in some limiting cases. The last section is devoted to a discussion of the transport properties close to the SI transition. In this chapter we will not discuss the effects of disorder. This may lead to an additional glass transition [39–41] as it will discussed by J.V. Josè in this volume.

II. THE MODELS

A quantum JJA consists of metallic islands (which undergo a superconducting transition of the BCS type at a transition temperatures T_c) which are connected by tunnel junctions. Each island has a capacitance to each of the other islands, to the ground and to any neighboring metallic region (such as gates or leads). The electrostatic energy of the system is entirely specified by the capacitance matrix C_{ij} [42] and the charge configuration $Q_i \equiv 2eq_i$ of each island (q_i being an integer number). Moreover, as known from the classical arrays, the Josephson coupling across the junctions introduces another contribution to the energy. Since at low temperatures the fluctuations of the amplitude of the order parameter can be ignored, the only relevant dynamical variables are the phases ϕ_i of each island, and the charge, Both are canonically conjugated variables [43]

$$[\phi_i, Q_j] = 2e \, i \, \delta_{ij}$$

Thus the relevant physics is captured by the following model, frequently defined as the Quantum Phase Model (QPM)

$$H_{\text{QPM}} = \sum_{i,j} (q_i - q_x) \, U_{ij} \, (q_j - q_x) - E_J \sum_{<i,j>} \cos \left(\phi_i - \phi_j - A_{ij} \right) . \tag{1}$$

The Coulomb interaction is described by the matrix $U_{ij} = e^2 C_{ij}^{-1}$. The simplest, sufficiently realistic, model for the capacitance matrix C_{ij} includes only the ground capacitance C_0 and the junction capacitance C, with the corresponding energy scales $E_C = e^2/2C$ and $E_0 = e^2/2C_0$. The range of the electrostatic interaction between Cooper pairs is , in units of the lattice spacing, $\lambda = \sqrt{C/C_0}$. A control (external) voltage V_x applied to the ground plane enters via the induced charge $Q_x = 2eq_x = \sum_j C_{ij} V_x$ (a homogeneous situation is considered here). When tuning V_x different charge configurations minimize the electrostatic energy. It suppresses tunneling (Coulomb blockade) except at degeneracy points. A perpendicular magnetic field with vector potential $\mathbf{A}$ enters the QPM in the standard way through $A_{ij} = 2e \int_i^j \mathbf{A} \cdot d\mathbf{l}$. The relevant parameter which describes the magnetic frustration is $f = (1/2\pi) \sum A_{ij}$, where the summation runs over an elementary plaquette.

The QPM accounts only for Cooper pair tunneling, in some case one has to take into account the tunneling of quasiparticles and/or the flow of Ohmic current through the substrate or between the junctions. These effects will be discussed in the section devoted to the transport properties.

In the case of strong *on-site* Coulomb interaction $U_{ii} = U_0$ and very low temperatures only few charge states are important. If the gate voltage is tuned close to a degeneracy, the relevant physics is captured by considering only two adjacent charge states of each island, and the QPM is equivalent to an anisotropic XXZ spin-1/2 Heisenberg model [20]

3

$$H_S = -h \sum_i S_i^z + \sum_{i,j} S_i^z U_{ij} S_j^z - E_J \sum_{\langle i,j \rangle} \left(e^{iA_{ij}} S_i^+ S_j^- + e^{-iA_{ij}} S_j^+ S_i^- \right) . \tag{2}$$

The operators S_i^z, S_i^+, S_j^- are the spin-1/2 operators, S_i^z being related to the charge on each island ($q_i = S_i^z + \frac{1}{2}$), and the raising and lowering $S_i^\pm$ operators corresponding to the "creation" and "annihilation" operators $e^{\pm i\phi_j}$ of the QPM. The "external" field h is related to the external charge by

$$h = (q_x - 1/2) \sum_j U_{ij} .$$

Various magnetic ordered phases of the XXZ Hamiltonian correspond to the different phases in the QPM. Long range order in $\langle S^+ \rangle$ indicates superfluidity in the QPM while long range order in $\langle S^z \rangle$ describes order in the charge configuration.

There is yet another closely related model which is mostly used in the context of superconductivity in ultrathin films, the Bose-Hubbard model [39]

$$H = \frac{1}{2} \sum_i n_i U_{ij} n_i - \mu \sum_i n_i - \frac{t}{2} \sum_{\langle ij \rangle} (b_i^\dagger b_j + h.c.) \tag{3}$$

where $b^\dagger$, b are the creation and annihilation operators for bosons and $n_i = b_i^\dagger b_i$ is the number of bosons. Again U_{ij} describes the Coulomb interaction between bosons, μ is the chemical potential, and t the hopping matrix element. The connection between the Bose-Hubbard model and the QPM is easily seen by writing the field b_i in terms of amplitude and phase and then approximating the amplitude by its average, i.e. $b_i \sim e^{i\phi_i}$. The hopping term is then associated with the Josephson tunneling while the chemical potential plays the same role as the external charge in the QPM. This mapping becomes more accurate as the average number of bosons per sites increases.

The three models are equivalent in the sense that they belong to the same universality class (they lead to the same Ginzburg-Landau effective free energy). However, the non-universal features like the location of the phase transitions depend quantitatively on the specific choice of the model.

III. ANALYTIC TOOLS

A. Mean Field

The mean field approximation consists in approximating the Hamiltonian of eq.(1) by [44,45]

$$H_{\mathrm{MF}} = \frac{1}{2} \sum_{i,j} q_i U_{ij} q_j - z E_J \langle \cos(\phi) \rangle \sum_j \cos(\phi_j)$$

where z is the coordination number in the lattice and $\psi \equiv \langle \cos(\phi) \rangle$ is the order parameter. It has to be calculated self-consistently according to

$$\langle \cos(\phi) \rangle = \mathrm{Tr} \left\{ \cos(\phi_i) \exp(-\beta H_{\mathrm{MF}}) \right\} / \mathrm{Tr} \left\{ \exp(-\beta H_{\mathrm{MF}}) \right\} .$$

Close to the transition point, the thermal average on the r.h.s can be evaluated by expanding in powers of ψ. To third order, a Ginzburg-Landau type equation arises:

4

$$\left[1 - zE_J \int_0^\beta d\tau \langle \cos\phi_i(\tau) \cos\phi_i(0) \rangle_{ch} \right] \psi + \left(\frac{zE_J}{U_0} \right)^3 \mathcal{B}\, \psi^3 = 0 \qquad (4)$$

Here the average $< ... >_{ch}$ is performed over the eigenstates of the charging part of the Hamiltonian only and the quantity $\mathcal{B}$ entails the four point phase correlation. If the charging term is absent, the phase-phase correlator in Eq. (4) is one and we recover the classical result $\beta_{cr} z E_J = 2$. Due to the charging effects the phase starts to fluctuate and the critical temperature is depressed. The correlator is easy to evaluate. For instance in the self-charging limit $U_{ij} = U_0 \delta_{ij}$ at $T = 0$ it is ($U_0 \equiv 8E_0$ only if the junction capacitance is zero).

$$\langle \cos\phi_i(\tau) \cos\phi_i(0) \rangle_{ch} = (1/2) \exp\{ -(U_0/2)\tau\, (1 - \tau/\beta) \}\ .$$

As a result the SI transition at zero temperature occurs at

$$2zE_J = U_0\ \ .$$

For larger values of the charging energy the array does not acquire phase coherence even at zero temperature. The full phase diagram will be described in details in the next section.

Similar types of mean field approaches can be used to study the effect of frustration in these systems. In this case, however, a nontrivial space dependence of the order parameter may arise.

B. Coarse-Graining approach

By using the coarse-graining approximation it is possible to go from the microscopic models introduced in the previous section to a Ginzburg-Landau effective free energy which depend only on the order parameter [47,48]. Since the transition in this case is governed by quantum fluctuations, the order parameter will depend both on space and (imaginary)-time [49].

The coarse-graining proceeds in two steps:

- An auxiliary field $\psi(x, \tau)$ (which has the meaning of an order parameter) is introduced through a Hubbard-Stratonovich transformation. The partition function is then expressed as a path integral over ψ.

- The assumption that the order parameter is small close to the transition allows a subsequent cumulant expansion to obtain the usual (polynomial) GL effective free energy. The coefficients depend on the details of the microscopic model.

The partition function of the QPM is given by

$$Z = Tr\{ e^{-\beta H_{QPM}} \} = Z_{ch} \langle T_\tau e^{-\int_0^\beta d\tau H_J(\tau)} \rangle \qquad (5)$$

where the subscripts ch and J indicate the charging and Josephson part to the Hamiltonian of Eq.(1). Applying the Hubbard-Stratonovich transformation to the Josephson term we get

$$\exp\left\{ \frac{E_J}{2} \int_0^\beta d\tau \sum_{\langle i,j \rangle} e^{i\phi_i} e^{-i\phi_j} + h.c. \right\}$$

$$\sim \int \mathcal{D}\psi^* \mathcal{D}\psi \exp\left\{-\int_0^\beta d\tau \sum_{\langle i,j\rangle} (E_{\mathrm{J}})_{ij}^{-1} \psi_i^*(\tau)\psi(\tau) + \int_0^\beta d\tau \sum_i \left[\psi_i^*(\tau)e^{i\phi_i(\tau)} + h.c.\right]\right\} \qquad (6)$$

Here we introduced a matrix $(E_{\mathrm{J}})_{ij}$ which is equal to E_{J} if ij are nearest neighbors and zero otherwise. Now the partition function can be written as

$$Z = Z_{\mathrm{ch}} \int \mathcal{D}\psi^* \mathcal{D}\psi \exp\left\{-F[\psi]\right\} \qquad (7)$$

where the effective free energy F is defined as

$$F = -\int_0^\beta d\tau \sum_{ij} (E_{\mathrm{J}})_{ij}^{-1} \psi_i^*(\tau)\psi(\tau) - \ln\left\langle -\int_0^\beta d\tau \sum_i \left[\psi_i^*(\tau)e^{i\phi_i(\tau)} + h.c.\right]\right\rangle_{\mathrm{ch}} . \qquad (8)$$

After truncation of higher order terms and a gradient expansion, the effective free energy reads

$$F = \int d^2r \, d\tau d\tau' \psi^*(r,\tau) \left\{ \frac{1}{2E_{\mathrm{J}}} \left[1 + \frac{1}{4}\left(\frac{\vec{\nabla}}{i} + \frac{2e}{\hbar}\vec{A}\right)^2 \right] - g(\tau - \tau') \right\} \psi(r,\tau')$$

$$+\kappa \int d^2r \, d\tau |\psi(r,\tau)|^4 . \qquad (9)$$

The dynamics of the field ψ is governed by the phase-phase correlator

$$g(\tau) = \left\langle \exp\{i\phi_i(\tau) - i\phi_i(0)\}\right\rangle_{\mathrm{ch}} ,$$

while κ depends on a 4-point phase correlator. The effect of a magnetic field and frustration can be introduced in the standard way by the replacement $\nabla \to \nabla + 2e\vec{A}$.

In the mean field approximation the phase transition is obtained for

$$\frac{1}{2E_{\mathrm{J}}} = \int_0^\beta d\tau g(\tau) . \qquad (10)$$

which coincides with the results of the previous section. In the coarse graining approach, however, a systematic treatment of the fluctuations is possible.

C. Duality Transformations

In this section we derive some properties of quantum JJA using dual transformations [50–53]. We follow closely the derivation given in Ref. [12]. Our starting point is the partition function expressed in terms of the Euclidean action [4],

$$Z = \prod_i \int_0^{2\pi} d\phi_i^{(0)} \sum_{\{m_i=0,\pm 1,\dots\}} \int_{\phi_i^{(0)}}^{\phi_i^{(0)}+2\pi m_i} D\phi_i(\tau) \exp[-S\{\phi\}] . \qquad (11)$$

Here the path integration is carried out with the boundary conditions

$$\phi_i(0) = \phi_i^{(0)}; \quad \phi_i(\beta) = \phi_i^{(0)} + 2\pi m_i, \qquad (12)$$

6

with β being the inverse temperature. These non-trivial boundary conditions express the fact that the charges of the grains are integer multiples of $2e$ [4]. The Euclidean effective action $S\{\phi\}$ has the form

$$S[\phi] = \int_0^\beta d\tau \left\{ \frac{C_0}{8e^2} \sum_i (\dot{\phi}_i)^2 + \frac{C}{8e^2} \sum_{\langle ij \rangle} (\dot{\phi}_i - \dot{\phi}_j)^2 - E_J \sum_{\langle ij \rangle} \cos(\phi_i - \phi_j) \right\}. \tag{13}$$

The first two terms are easily recognized to be charging energy expressed in terms of voltages ($\phi = 2eV_i$). It is clear that when the Josephson energy is either much larger or much smaller than the charging energy, the properties of the array are governed either by vortices or charges. It is therefore useful to express the action of the system in terms of these degrees of freedom. Vortex degrees of freedom have been introduced in the classical limit by means of the Villain transformation [54]; the quantum problem requires some additional steps [12]. We introduce the lattice with spacing ϵ in time direction; this spacing is of order of inverse Josephson plasmon frequency, $\epsilon \sim (8E_J E_C)^{1/2}$. In the Villain approximation one replaces

$$\exp\left\{ -\epsilon E_J \sum_{\langle ij \rangle, \tau} [1 - \cos(\phi_{i,\tau} - \phi_{j,\tau})] \right\} \to \sum_{\{\mathbf{m}_{i\tau}\}} \exp\left\{ -\frac{\epsilon E_J}{2} \sum_{i,\tau} |\nabla \phi_{i\tau} - 2\pi \mathbf{m}_{i\tau}|^2 \right\}.$$

A resummation of the expression on the r.h.s. yields

$$\sum_{\{\mathbf{J}_{i\tau}\}} \exp\left\{ -\frac{1}{2\epsilon E_J} \sum_{i,\tau} |\mathbf{J}_{i\tau}|^2 - i\mathbf{J}_{i\tau} \nabla \phi_{i\tau} \right\}.$$

After this step the Gaussian integration over the phases can be performed, with the result

$$Z = \sum_{q_{i\tau}} \sum_{\mathbf{J}_{i\tau}} \exp\left\{ -\epsilon \sum_{i,j,\tau} q_{i\tau} U_{ij} q_{j\tau} - \frac{1}{2\epsilon E_J} \sum_{i,\tau} |\mathbf{J}_{i\tau}|^2 \right\}. \tag{14}$$

The summation is constrained by the continuity equation,

$$\nabla \mathbf{J}_{i\tau} - \dot{q}_{i\tau} = 0 .$$

Here and in the following the time derivative stands for a discrete derivative $\dot{f}(\tau) = \epsilon_\mu^{-1}[f(\tau + \epsilon_\mu) - f(\tau)]$. The constraint is satisfied by the parameterization [55]

$$J_{i\tau}^{(\mu)} = n^{(\mu)} (\mathbf{n}\nabla)^{-1} \dot{q}_{i\tau} + \epsilon^{(\mu\nu)} \nabla_\nu A_{i\tau} ,$$

where $A_{i\tau}$ is an unconstrained integer-valued scalar field. The operator $(\mathbf{n}\nabla)^{-1}$ is the line integral on the lattice (in Fourier space it has the form $i(k_x + k_y)^{-1}$), while $\epsilon^{(\mu\nu)}$ is the antisymmetric tensor.

With the use of the Poisson resummation (which requires introducing a new integer scalar field $v_{i\tau}$) the partition function can be written as a sume over two integer valued fields defined on the space-time lattice, the charges $q_{i\tau}$ and vorticities $v_{i\tau}$,

$$Z = \sum_{q_{i\tau}, v_{i\tau}} \exp -S\{q, v\} .$$

The effective action is

$$S\{q,v\} = \int_0^\beta d\tau \sum_{ij} \left\{ 2e^2 q_{i\tau} U_{ij} q_{j\tau} + \pi E_{\mathrm{J}} v_{i\tau} G_{ij} v_{j\tau} + i q_{i\tau} \Theta_{ij} \dot{v}_{j\tau} + \frac{1}{4\pi E_{\mathrm{J}}} \dot{q}_{i\tau} G_{ij} \dot{q}_{j\tau} \right\}. \qquad (15)$$

It describes two coupled Coulomb gases. The charges interact via the inverse capacitance matrix. The interaction among the vortices is described by the kernel G_{ij}, which is obtained as the Fourier transform of k^{-2}. At large distances $r_{ij} \gg a$ between the sites i and j it depends logarithmically on the distance

$$G_{ij} = \frac{1}{2} \ln\left(\frac{a}{r_{ij}}\right).$$

The charges and vortices are coupled in the dynamical theory as described by the third term. Here

$$\Theta_{ij} = \arctan\left(\frac{y_i - y_j}{x_i - x_j}\right)$$

describes the phase configuration at the site i if a vortex is placed at the site j. The coupling has a simple physical interpretation: a change of vorticity at site j produces a voltage at site i which is felt by the charge at this location. The last term $\dot{q}G\dot{q}$ represents a spin-wave contribution to the charge correlation function.

The effective action (15) shows a high degree of symmetry between vortex and charge degrees of freedom. In particular, in the limit $C_0 \ll C$ the inverse capacitance matrix has the same functional form as the kernel describing the vortex interaction, $e^2 C_{ij}^{-1} = E_{\mathrm{C}} G_{ij}/\pi$, and the charges and vortices are (approximately) dual. The duality is broken by the last term $\dot{q}G\dot{q}$. This term is "irrelevant" for the phase transitions, i.e. it merely shifts the transition point. However, it has important implications for the dynamical behavior.

Recently the same duality transformations has been applied to double layers [13]. They will be reviewed by J.V. Josè in this volume.

IV. THE PHASE DIAGRAM

The phase diagram in quantum JJA depends sensitively on the exact model considered. Moreover in the presence of charge and/or magnetic frustration the boundaries changes and new phases appear. This section is organized in small subsections which briefly describe the main features of the phase diagram in various limiting cases.

A. Long range Coulomb interaction, $C \gg C_0$

At transition temperature the vortex-unbinding KTB transition, from the superconducting to the resistive phase, is shifted by quantum fluctuations to values below the transition temperature T_{J} of the classical array (with $E_{\mathrm{C}} = 0$). In the case $C_0 = 0$ the shift of the transition temperature is [56]

$$T_{\mathrm{J}} = \frac{\pi E_{\mathrm{J}}}{2} - \frac{E_{\mathrm{C}}}{6}. \qquad (16)$$

If $C \gg C_0$ another phase transition occurs at finite temperature [57]. In this limit charges interact logarithmically. Hnece they undergo a charge-unbinding KTB transition, which now separates an insulating low-temperature phase from a conducting high-temperature phase. In the limit of weak Josephson coupling the charge-KTB transition occur at a temperature [12]

$$T_{\mathrm{C}} = \frac{E_{\mathrm{C}}}{\pi} - 0.31\frac{(E_{\mathrm{J}})^2}{E_{\mathrm{C}}} \ .$$

Hence the array has three different phases. Upon increasing the charging energy the system undergoes first a superconducting - resistive transition and then a resistive – insulating transition. At $T = 0$ there is a direct superconducting – insulator transition which occurs at a critical point

$$\frac{E_{\mathrm{J}}}{E_{\mathrm{C}}} \sim \frac{2}{\pi^2}$$

At this critical point the system is self-dual with respect to interchanging of charges and vortices. The duality is strict only in the ideal case of vanishing self-capacitance and the absence of the spin-wave duality breaking term in eq. (15). The phase diagram corresponding to this case is shown in Fig.(1). Experimental evidence of this behavior has been found van der Zant *et al.* [6,58].

B. Short range Coulomb interaction, $C \ll C_0$

In this case the phase boundary can be obtained using the mean field theory. The phase – phase correlator needed in Eq. (10) can be easily calculated for a general capacitance matrix [46]. In Fig. 2 we show the phase diagram for the self-charging model ($C = 0$) as a function of the external charge q_x at zero temperature. As a function of q_{x} a lobe structure appears. A finite external charge lowers the energy cost to transfer Cooper pairs between neighboring grains, increasing the regime of the superconducting phase. At the degeneracy points the superconducting phase extends to down to arbitrary small Josephson couplings.

For finite-range Coulomb interaction, further insulating phases are stable, and the phase diagram becomes rather rich. In this case not only Mott-insulating phases with the same integer filling of each island are allowed, but new lobes with crystal-like structure of the filling, e.g. $q_i = 0$ or 1 arise. The simplest is a checkerboard pattern with alternating filling of neighboring islands. In general, with increasing external charge, a sequence of inhomogeneous charge configurations minimizes the energy. Since the Mott-insulating lobes are incompressible (there is a gap in the excitation spectrum), the average charge $\langle q \rangle$ is pinned to a fractional value in the whole lobe. In Fig.3 a schematic phase diagram is shown, where on-site U_0 and nearest neighboring U_1 Coulomb interaction are taken into account. In this case the only fractional filling which can occur is the checkerboard configuration with $\langle q \rangle = 1/2$. At finite temperature the thermal occupation of higher charges states smears the lobe structure [46,59].

The combined effect of Josephson coupling and finite range interaction with charge frustration leads to the possibility of new phases, called *supersolids*. The concept of supersolids dates back to the early 70's when Andreev and Lifshitz [18] proposed that vacancies in a quantum crystal might undergo a Bose-Einstein condensation without destroying the crystal order. In such a phase the superfluid order and the crystalline order coexist.

The exciting possibility of a supersolid phase in Josephson junction arrays and Bose-Hubbard systems has been extensively investigated in recent years. Loosely speaking, the supersolid phase is located in an intermediate region around the half-filling lobe. A simple way to understand its existence is to focus on a region close to the phase boundary at $q_x \sim 1/2$. In this case there will be a finite density of vacancies. They have bosonic character and therefore have the possibility to Bose condense. In a limited range of parameters they can become superfluid (and therefore are able to move freely through the system) without being able to destroy completely the crystal order (since they have a low density).

There are various methods to study the supersolid phase in JJA. We follow here a variational approach discussed in Ref. [60] (valid only at zero temperature). The idea is to consider a variational wave function of the Gutzwiller type, as discussed in early treatments of spin [61] and Bose-Hubbard [62] models. It is convenient to write down the variational ground state using as a basis the charge on each island ($\mid q_i \rangle$). For simplicity we choose it as a product of single-site wave functions

$$\mid G_0 \rangle = Z^{-1} \prod_{n=1}^{\infty} \sum_{[n_i]} e^{-k_i(q_i - m_i)^2/2} \mid q_i \rangle \,, \tag{17}$$

where k_i and m_i are variational parameters, and Z is a normalization constant. In the limit of zero charging energy, each island of the array has a fixed phase ϕ, this corresponds to a coherent superpositions of charge states, i.e. $k_i = 0$ in the variational wave function. In the case of non-zero charging energy, states in which the islands have non-zero charge are suppressed. This effect is controlled by the variational parameter k. The other variational parameter m fixes the average charge on each island.

The variational parameters are determined by minimizing the energy expectation value $E_{QPM} = \langle G_0 \mid H_{QPM} \mid G_0 \rangle$. The various phases are determined by evaluating the average of the superconducting order

$$\psi_i = \langle G_0 \mid e^{i\phi_i} \mid G_0 \rangle \,,$$

and the structure factor (which signals crystal order)

$$S(\pi, \pi) = \frac{1}{N^2} \langle G_0 \mid \sum_{n=a,j} (-1)^{|i-j|} q_i q_j \mid G_0 \rangle \,.$$

A finite $S(\pi, \pi)$ corresponds to a checkerboard arrangement of the charges on the islands. Due to discrete sums required in the evaluation of the expectation values the calculation should be done numerically. Results are shown in Fig. 4.

V. TRANSPORT PROPERTIES

In two dimensions at the SI transition at $T = 0$ the conductance has been predicted to be finite and universal [27,28]. This is quite striking since a metallic behavior should be present even in the absence of dissipation. This effect is entirely due to the presence of collective modes which become critical at the transition point. The prediction of a metallic behavior at zero temperature created a lot of interest both on the experimental and the theoretical side. The universal conductance in a model with no disorder was considered in Ref. [30]

by means of $1/N$ expansion [63] and Monte Carlo simulations and in Ref. [37] by means of an ϵ-expansion [63]. The dirty boson system and the transition to the Bose glass phase (including the case of long-range Coulomb interaction) was extensively studied in [35,31]. Wen employed a scaling theory of conserved currents at anisotropic critical points [64] identifying many universal amplitudes. One of these amplitudes in two dimensions reduces to the universal conductance $\sigma^\star$. The finite frequencies properties close to the transition point were analyzed by means of the $1/N$ expansion [33,34]. On the numerical side, besides the Monte Carlo simulations, exact diagonalization calculation [36] were employed to evaluate the universal value of the conductivity $\sigma^\star$.

The simplest way to evaluate the conductivity is to use the Ginzburg-Landau formulation of Eq.(9) in imaginary time and then to continue the result analytically to real times. The conductivity in the linear response regime can be determined from the functional derivatives of the partition function. Noticing that the current is the derivative of the free energy with respect to the vector potential and that the electric field is the time derivative of the vector potential (with a negative sign), the conductivity is expressed as

$$\sigma_{ab}(\omega_\mu) = \frac{\hbar}{\omega_\mu} \int d^2r\, d\tau \frac{\delta^2 \ln Z}{\delta A_a(r,\tau)\delta A_b(0)}\Big|_{\vec{A}=0} e^{i\omega_\mu \tau} \ . \tag{18}$$

Using Eq.(9), the longitudinal conductivity $\sigma_{aa}(\omega_\mu)$ can be expressed in terms of two- and four-point Green's functions. In the absence of a magnetic field we have [30]

$$\sigma(\omega_\mu) = \frac{4\pi}{R_Q \omega_\mu}\Big[\int \frac{d^3q}{(2\pi)^3}\langle \psi_{\vec{q}}^* \psi_{\vec{q}}\rangle - 2\int \frac{d^3q\, d^3p}{(2\pi)^6} q_x p_x \langle \psi_{\vec{q}-\frac{\vec{k}}{2}}^* \psi_{\vec{p}+\frac{\vec{k}}{2}}^* \psi_{\vec{p}-\frac{\vec{k}}{2}} \psi_{\vec{q}+\frac{\vec{k}}{2}}\rangle\Big] \tag{19}$$

where the $\vec{q} = (q_x, q_y, \omega_\nu)$ are vectors in the 3-dimensional space-time, $\vec{k} = (0, 0, \omega_\mu)$ and $R_Q = h/4e^2$. There are various approaches to evaluate these correlators. The most straightforward is the Gaussian approximation which turns out to be the first term in a $1/N$ expansion [30]. Evaluating the correlators with the quadratic part of the free energy one gets

$$\sigma(\omega_\mu) = \frac{1}{R_Q \omega_\mu}\frac{1}{\beta}\sum_\nu \int dk\, k^3\, G(k,\omega_\nu)\,[G(k,\omega_\nu) - G(k,\omega_\nu + \omega_\mu)] \ ,$$

where $G(k,\omega_\mu) = [\epsilon + k^2 + \zeta\omega_\mu^2]^{-1}$. Performing the k-integrals and the analytical continuation to real frequencies, the real and imaginary parts of the conductivity are

$$\Re\,\sigma(\omega) = \frac{\pi}{8R_Q}\left(1 - \frac{\omega_c^2}{\omega^2}\right)\Theta(\omega_c^2 - \omega^2) \tag{20}$$

$$\Im\,\sigma(\omega) = \frac{1}{8R_Q}\left[-\frac{2\omega_c}{\omega}\left(1 - \frac{\omega_c^2}{\omega^2}\right)\ln\left|\frac{\omega - \omega_c}{\omega + \omega_c}\right|\right] \tag{21}$$

The threshold is $\omega_c = 8U_0\sqrt{(1 - E_J/U_0)}$ (in the case of on-site interaction). It vanishes at the SI transition thus leading to a finite d.c. $(\omega \to 0)$ conductivity,

$$\sigma^\star = \frac{\pi}{8}\frac{4e^2}{h} \ . \tag{22}$$

11

Corrections to the next order in the $1/N$ expansion correct the Gaussian result by roughly 30% yielding $\sigma^\star \sim 0.251\sigma_Q$. Another powerful method for evaluating critical quantities is the ϵ-expansion [63]. In order to set up the ϵ-expansion one should move away from two-dimensions and consider systems with $d-1$ spatial dimensions. Eq. (19) should be rewritten accordingly (i.e. the three-dimensional vectors should be replaced by d-dimensional ones). This approach allows also to obtain the scaling form of the frequency dependent conductance (for more details the interested reader is referred to Ref. [37]). In two dimension, to order ϵ^2, the universal conductance is

$$\sigma^\star = 0.315\frac{4e^2}{h} \ . \tag{23}$$

slightly larger than the result of the Monte Carlo simulation of Ref. [30].

The question arises how a system of bosons can have a dissipative dynamics at zero temperature. A look at the available experiments shows indeed a finite conductance at zero temperature, however, its value appears not to be universal. The origin of the dissipative dynamics may be Ohmic shunts or quasi-particle tunneling between the islands, which been studied extensively in the past (see e.g. Ref. [67]). Pair breaking processes are another mechanism for damping. These processes are present in inhomogeneous films if the order parameter is locally suppressed, or due to Andreev scattering at the boundaries of the grains. Dissipation may arise also due to electronic degrees of freedom, which can be introduced in the model of Eq.(1) by means of what is know as the 'local damping' model. Local damping changes the universality class of the SI transition [29], it also has been known to influence the low frequency dispersion of the vortex response in classical arrays [65,66].

In the presence of Ohmic shunts the effective Euclidean action (13)) for the array gets the additional contribution

$$S_{LD}[\phi] = \frac{1}{2}\int_0^\beta d\tau d\tau' \sum_{ij} \alpha_{ij}(\tau - \tau')\left[\phi_i(\tau) - \phi_j(\tau')\right]^2 \ . \tag{24}$$

For Ohmic baths the Fourier transform of the kernel is $\alpha_{ij}(\omega_\mu) = |\omega_\mu|(\alpha_0 + \alpha_1 k^2)/2\pi$. In this general expression shunts to the ground ($\alpha_0 = R_Q/R_0$) and shunts between the islands ($\alpha_1 = R_Q/R$) are accounted for. The shunts break the 2π-periodicity in the phase variables since they allow for continuous charge fluctuations. The *local* Ohmic damping (the term proportional to α_0) correlates the phase of a single island at different times. In proximity-coupled arrays, which consist of superconducting islands on top of a metallic film, the model with local damping is appropriate to describe the flow of normal electrons into the substrate. This process induces a dissipation for the phase ϕ_i, rather than for the phase difference $\phi_i - \phi_j$ as in the resistively shunted junctions (RSJ) model. The number of Cooper pairs in each island is allowed to decay in the presence of a local damping, whereas the RSJ model describes only charge transfer between neighboring islands.

By going over the same steps outlined in the section on the coarse graining, it is possible to obtain also in this case an effective Ginzburg-Landau free energy. The only difference is that now the phase-phase correlator $g(\tau)$ has to be evaluated including the local damping term. For small frequencies the Fourier transform reads (for more details see Ref. [29])

$$g(\omega_\mu) = g(0) - \eta\,|\omega_\mu|^s - \zeta\omega_\mu^2 \qquad \text{with } s = \frac{2}{\alpha} - 1 \ . \tag{25}$$

The coefficients η and ζ can be determined from the phase correlator, their value is not important for our purposes. Using this expression for $g(\omega_\mu)$, the free energy (9) contains a *non-Ohmic* dissipative term ($\propto |\omega_\mu|^s$) (reducing to Ohmic, or 'velocity proportional' damping only in the special case $s = 1$). This means that an *Ohmic* damping in the quantum phase model yields a *non-Ohmic* dynamics for the coarse-grained order-parameter.

The phase boundary in the saddle point approximation is shown in the inset of Fig. 5. Increasing damping shifts the phase boundary to smaller values of E_J. At $T = 0$ a quantum phase transition is ruled out beyond the critical value $\alpha = 2$. The value of the d.c. conductivity *at the transition* is displayed in Fig. 4. The non-dissipative transition has a *finite basin of attraction*: $0 \leq \alpha_0 \leq 2/3$. Here the dissipation is an irrelevant operator, and the transition is characterized by $z = 1$ and a universal critical conductivity. However, for stronger damping $\alpha_0 > 2/3$ a new universality class describes the transition, with a *damping dependent* conductance σ^* and $z = 2/s$ as observed experimentally.

ACKNOWLEDGMENTS

REFERENCES

[1] Proceedings of the NATO Advanced Research Workshop on *Coherence in superconducting networks*, J.E. Mooij and G.Schön Eds., Physica B **152** (1988).

[2] J.E. Mooij and G. Schön in *Single Charge tunneling* H. Grabert and M.H. Devoret Eds., NATO ASI series Vol.294 (Plenum, NY 1992), p. 275.

[3] Proc. of the Conference on *Macroscopic quantum phenomena and coherence in superconducting networks* C. Giovannella and M. Tinkham Eds., World Scientific (Singapore, 1995).

[4] G. Schön and A.D. Zaikin, Phys. Rep. **198**, 237 (1990).

[5] L.J. Geerligs, M. Peters, L.E.M. de Groot, A. Verbruggen, and J.E. Mooij, Phys. Rev. Lett. **63**, 326 (1989).

[6] H.S.J. van der Zant, L.J. Geerligs, and J.E. Mooij, Europhys. Lett. **19**, 541 (1992).

[7] C.D. Chen, P. Delsing, D.B. Haviland, Y.Harada, and T. Claeson, Phys. Rev. B **50**, 3959 (1995).

[8] R. Yagi, T. Tamaguchi, H. Kazawa and S. Kobayashi, J. Phys. Soc. Jpn. **65**, 36 (1996). Very recently the same group has studied the SI transition also in JJA, R. Yagi, T. Tamaguchi, H. Kazawa and S. Kobayashi, J. Phys. Soc. Jpn. **66**, 2429 (1997).

[9] D.B. Haviland, Y. Liu, and A.M. Goldman, Phys. Rev. Lett. **62**, 2180 (1989).

[10] A. Hebard and M. Palaanen, Phys. Rev. Lett.**65**, 927 (1990).

[11] S.L. Sondhi, S.M. Girvin, J.P. Carini, and S. Shahar, Rev. Mod. Phys. **69**, 315 (1997).

[12] R.Fazio and G. Schön, Phys. Rev. B **43**, 5307 (1991).

[13] Ya. Blanter and G. Schön, Phys. Rev. B **53**, 14534 (1996). Ya. Blanter, R.Fazio and G. Schön, Nucl. Phys. B **58**, 79 (1997).

[14] R.S. Fishman, and D. Stroud, Phys. Rev. B **37**, 1499 (1987).

[15] A. Kampf and G. Schön, Phys. Rev. B **37**, 5954 (1988).

[16] S. Teitel and C. Jayaprakash, Phys. Rev. B **27**, 598 (1983); S. Teitel and C. Jayaprakash, Phys. Rev. Lett. **51**, 1999 (1983); T.C. Halsey, Phys. Rev. B **31**, 5728 (1985); W. Y. Shih and D. Stroud, Phys. Rev. B **30**, 6774 (1984); W. Y. Shih and D. Stroud, Phys. Rev. B **28**, 6575 (1983); D. Ariosa, A. Vallat and H. Beck, J. Phys. France **51**, (1990).

[17] C. Bruder, R. Fazio, and G. Schön, Phys. Rev. B **47**, 342 (1993).

[18] A.F. Andreev, I.M. Lifshitz, Sov.Phys. *JETP* **29**, 1107 (1969).

[19] H. Matsuda and T. Tsuneto, Suppl. Prog. Theor. Phys. **46**, 411 (1970).

[20] K.S. Liu and M.E. Fisher, J. Low Temp. Phys. **10**, 655 (1973).

[21] E. Roddick and D.H. Stroud, Phys. Rev. B **48**, 16600 (1993); E. Sørensen and E. Roddick, Phys. Rev. B **53**, 8867 (1995).

[22] A. van Otterlo, K-H. Wagenblast, Phys. Rev. Lett. **48**, 16600 (1994).

[23] R.T. Scalettar, G.G. Batrouni, A.P. Kampf, G.T. Zimanyi Phys. Rev. B **51**, 8467 (1995).

[24] E. Frey and L. Balents, Phys. Rev. B **55**, 1050 (1997).

[25] L. Amico, G. Falci, R. Fazio, and G. Giaquinta, Phys. Rev. B **55**, 1100 (1997).

[26] A. Stern Phys. Rev. B **50**, 10092 (1994).; A.A. Odintsov and Yu. N. Nazarov, Phys. Rev. B **51**, 1133 (1995).; M.Y. Choi Phys. Rev. B **50**, 10088 (1994).

[27] M.P.A. Fisher, G. Grinstein and S.M. Girvin, Phys. Rev. Lett. **64**, 587 (1990).

[28] X.G. Wen and A. Zee, Int.J.Mod.Phys. B **4**, 437 (1990).

[29] K.-H. Wagenblast, A. van Otterlo, G.T. Zimanyi and G. Schön, Phys. Rev. Lett. **78**, 1779 (1997); ibid. **79**, 2730 (1997).

[30] M.-C. Cha, M.P.A. Fisher, S.M. Girvin, M. Wallin, A.P. Young, Phys. Rev. B **44**, 6883 (1991).

[31] E.S. Sørensen, M. Wallin, S.M. Girvin, and A.P. Young, Phys. Rev. Lett. **69**, 828 (1992).

[32] M. Wallin, E.S. Sørensen, S.M. Girvin, and A.P. Young, Phys. Rev. B **45**, 13136 (1992).

[33] A. van Otterlo, K.-H. Wagenblast, R. Fazio, and G. Schön, Phys. Rev. **48**, 3316 (1993).

[34] A.P. Kampf and G. T. Zimanyi, Phys. Rev. **47**, 279 (1993).

[35] G.G. Batrouni, B. Larson, R.T. Scalettar, J. Tobochnik, and J. Wang, Phys. Rev. B **48**, 9628 (1993).

[36] K. Runge, Phys. Rev. B **49**, 12115 (1994).

[37] R. Fazio and D. Zappalà, Phys. Rev. B **53**, R8883 (1996).

[38] K. Damle and S. Sachdev, cond-mat.9705206

[39] M.P.A. Fisher, B. P. Weichman, G. Grinstein, and D. S. Fisher, Phys. Rev. B **40**, 546 (1989).

[40] G. G. Batrouni, R. T. Scalettar, and G. T. Zimanyi, Phys. Rev. Lett. **65**, 1765 (1990).

[41] W. Krauth and N. Trivedi, Europhys. Lett. **14**, 627 (1991).

[42] J. D. Jackson, *Classical Electrodynamics*, John Wiley & Sons, 1975.

[43] P.W. Anderson, *Lectures on the Many Body Problem*, Caianiello Ed., Academic Press (New York, 1964), p.113.

[44] K.B. Efetov Sov. Phys. JETP **51**, 1015 (1980).

[45] E. Simanek, Phys. Rev. B **23**, 5762 (1982).

[46] C. Bruder, R. Fazio, A. Kampf, A. van Otterlo and G. Schön, Physica Scripta **T42**, 159 (1992).

[47] S. Doniach, Phys. Rev. B **24**, 5063 (1981).

[48] J.G. Kissner and U. Eckern, Z. Phys. **B91**, 155 (1993)

[49] J.A. Herz, Phys. Rev. B **14**, 1165 (1976).

[50] J. V. José, L. P. Kadanoff, S. Kirkpatrick, and D. R. Nelson, Phys. Rev. B **16**, 1217 (1977).

[51] L. P. Kadanoff, J. Phys. A **11**, 1399 (1978).

[52] R. Savit, Rev. Mod. Phys. **52**, 453 (1980).

[53] B. Nienhuis, in: *Phase transitions and critical phenomena*, Vol. 11, ed. by C. Domb and J. L. Lebowitz (Academic Press, London, 1987)., p.1.

[54] J. Villain, J.Physique **36**, 581 (1975).

[55] S. Elitzur, R. Pearson, and J. Shigemitzu, Phys. Rev. D **19**, 3638 (1979).

[56] J. V. José and C. Rojas, Physica B **203**, 481 (1994).

[57] J.E. Mooij, B.J. van Wees, L.J. Geerligs, M. Peters, R. Fazio, and G. Schön, Phys. Rev. Lett. **65**, 315 (1990).

[58] R. Yagi, T. Tamaguchi, H. Kazawa and S. Kobayashi, J. Phys. Soc. Jpn. **66**, 2429 (1997).

[59] B.-J. Kim, J. Kim, S.-Y Park and M.Y. Choi, cond-mat 9704176

[60] A. van Otterlo, K.-H. Wagenblast, R. Baltin, C. Bruder, R. Fazio, and G. Schön, Phys. Rev. **52**, 16176 (1995).

[61] D.A. Huse and V. Elser, Phys. Rev. Lett. **60**, 2351 (1988).

[62] W. Krauth, D. Caffarel, and J.-P. Bouchard, Phys. Rev. **45**, 3137 (1992).

[63] C. Itzykson and J.-M. Drouffe, *Statistical Field Theory*, Cambridge University Press (1989).

[64] X.G. Wen, Phys. Rev. B **46**, 2655 (1992).

[65] H. Beck, Phys. Rev. B **49**, 6153 (1994).

[66] S.E. Korshunov, Phys. Rev. B **50**, 13616 (1994).

[67] S. Chakravarty, G.-L. Ingold, S. Kivelson, and G.T. Zimanyi, Phys. Rev.B **37**, 3283 (1988) and references therein.
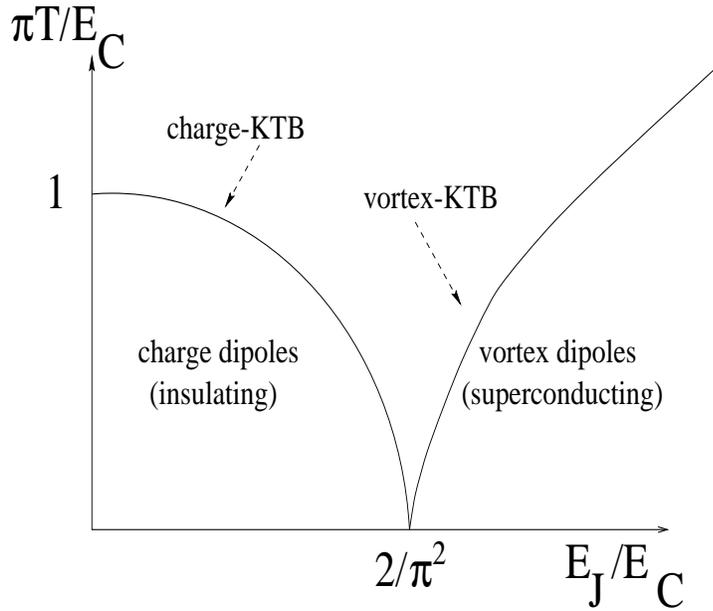
$\pi T/E_C$

charge-KTB

vortex-KTB

1

charge dipoles
(insulating)

vortex dipoles
(superconducting)

$2/\pi^2$

E_J/E_C

FIG. 1. The phase diagram for a quantum JJA in the limit of long range (logarithmic) interaction between charges.

q_x

2

Mott
insul.

1

superconductor

0

-

E_J/U_0
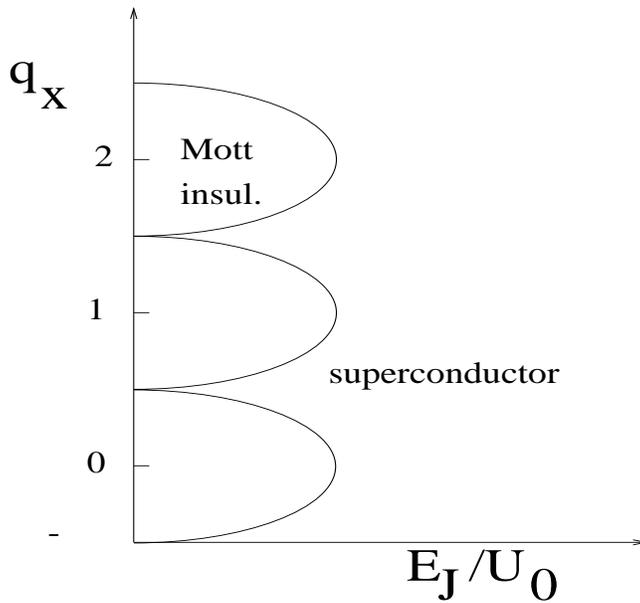
FIG. 2. The $T = 0$ phase diagram in the limit of on-site interaction as a function of the charge frustration. At the values of q_x for which two charge states are degenerate, the superconducting phase extends to arbitrary small Josephson coupling.
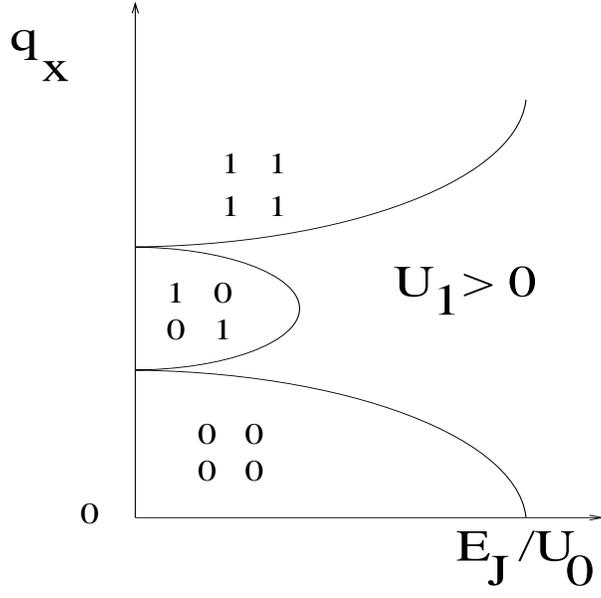
FIG. 3. The same as in Fig. 2 including a small rearest neighbor charging term U_1. Around $q_x = 1/2$ the half-integer lobe appears.
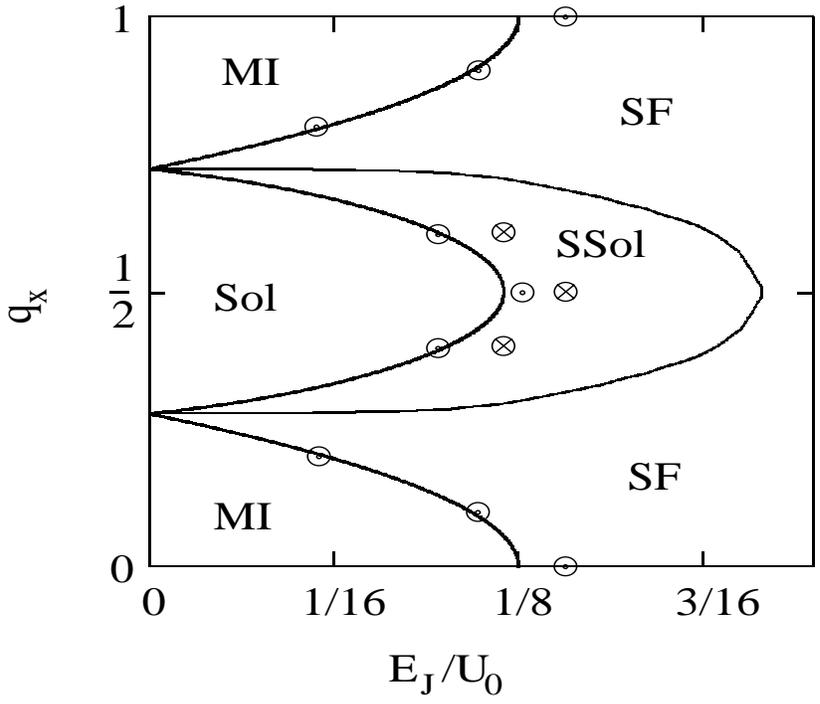

FIG. 4. The phase diagram as obtained from the variational calculation. Mi= Mott insulator, Sol = solid (with a chekerboard structure), SF = superfluid, Ssol = supersolid. ($U_1/U_0 = 0.2$
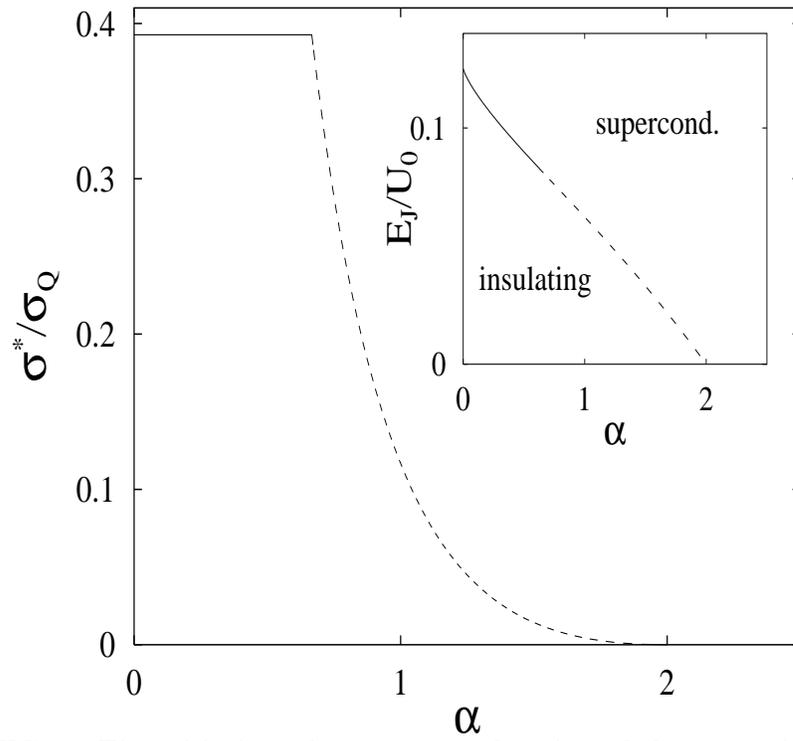
18

FIG. 5. The critical conductance as a function of the strength of the local damping. In the inset the SI phase boundary in the presence of dissipation.